Cell Reports

Report

Fanconi-Anemia-Associated Mutations Destabilize RAD51 Filaments and Impair Replication Fork Protection

Graphical Abstract

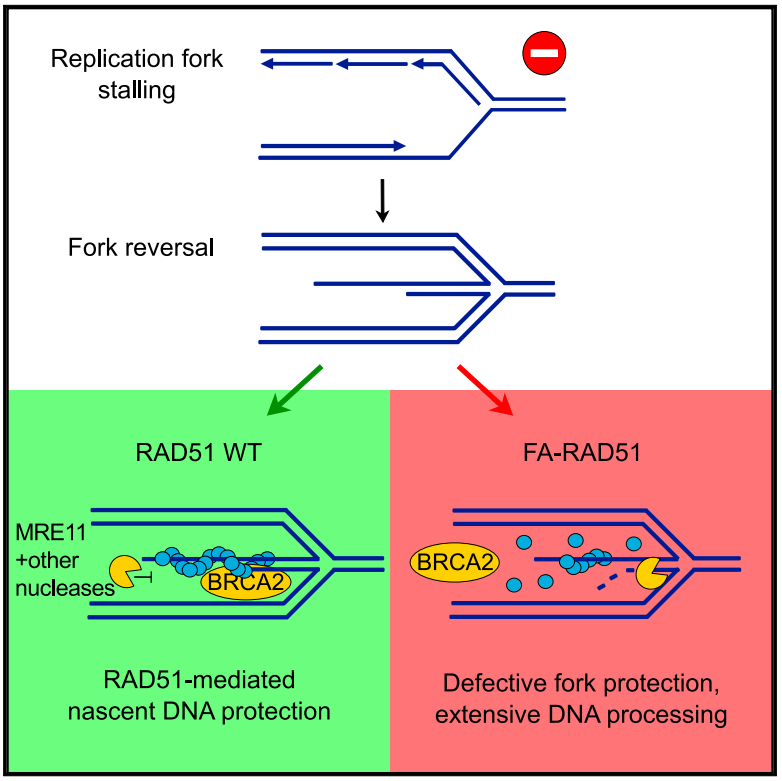

Authors

Karina Zadorozhny, Vincenzo Sannino, Ondrej Beláň, Jarmila Mlčoušková, Mário Špírek, Vincenzo Costanzo, Lumír Krejčí

Correspondence

vincenzo.costanzo@ifom.eu (V.C.), lkrejci@chemi.muni.cz (L.K.)

In Brief

Zadorozhny et al. find that RAD51 mutations associated with Fanconi anemia not only impair DNA crosslink repair but also affect DNA replication during fork stalling. The mutant proteins cause RAD51 filament destabilization and induce pronounced structural changes resulting from aberrant ATP binding and hydrolysis.

Highlights

- FA-associated RAD51 mutants are defective at stalled fork protection
- Structural properties of the RAD51 nucleoprotein filament are altered by FA mutations
- These filaments are highly unstable due to aberrant ATP binding and hydrolysis

Zadorozhny et al., 2017, Cell Reports *21*, 333–340
October 10, 2017
https://doi.org/10.1016/j.celrep.2017.09.062

CellPress

Cell Reports
Report

Fanconi-Anemia-Associated Mutations Destabilize RAD51 Filaments and Impair Replication Fork Protection

Karina Zadorozhny,[1] Vincenzo Sannino,[2] Ondrej Beláň,[1] Jarmila Mlčoušková,[1,3] Mário Špírek,[1,3] Vincenzo Costanzo,[2,*] and Lumír Krejčí[1,3,4,5,*]
[1]Department of Biology, Masaryk University, 62500 Brno, Czech Republic
[2]DNA Metabolism Laboratory, IFOM-The Firc Institute of Molecular Oncology, 20139 Milan, Italy
[3]International Clinical Research Center, St. Anne's University Hospital, 656 91 Brno, Czech Republic
[4]National Centre for Biomolecular Research, Masaryk University, 62500 Brno, Czech Republic
[5]Lead Contact
*Correspondence: vincenzo.costanzo@ifom.eu (V.C.), lkrejci@chemi.muni.cz (L.K.)
https://doi.org/10.1016/j.celrep.2017.09.062

SUMMARY

Fanconi anemia (FA) is a genetic disorder characterized by a defect in DNA interstrand crosslink (ICL) repair, chromosomal instability, and a predisposition to cancer. Recently, two RAD51 mutations were reported to cause an FA-like phenotype. Despite the tight association of FA/HR proteins with replication fork (RF) stabilization during normal replication, it remains unknown how FA-associated RAD51 mutations affect replication beyond ICL lesions. Here, we report that these mutations fail to protect nascent DNA from MRE11-mediated degradation during RF stalling in *Xenopus laevis* egg extracts. Reconstitution of DNA protection in vitro revealed that the defect arises directly due to altered RAD51 properties. Both mutations induce pronounced structural changes and RAD51 filament destabilization that is not rescued by prevention of ATP hydrolysis due to aberrant ATP binding. Our results further interconnect the FA pathway with DNA replication and provide mechanistic insight into the role of RAD51 in recombination-independent mechanisms of genome maintenance.

INTRODUCTION

Fanconi anemia (FA) is an autosomal recessive genetic disorder characterized by severe developmental abnormalities, chromosomal instability, bone marrow failure, and a high predisposition to a variety of cancer types. The FA pathway, currently involving 19 genes, coordinates a complex interstrand crosslink (ICL) repair mechanism that predominantly operates during DNA replication (Ceccaldi et al., 2016). The current model of ICL repair comprises nucleolytic incision of the lesion, resulting in the formation of a double-strand break. The broken replication fork (RF) is subsequently restored by homologous recombination (HR), characterized by an initial end-resection step followed by a homology search and D-loop formation mediated by RAD51, a central mammalian recombinase (Long et al., 2011; Räschle et al., 2008).

Recently, a recombination-independent role of RAD51 during ICL repair was described, as FA-patient-derived cells carrying RAD51 T131P mutations are hypersensitive to crosslinking agents but remain HR proficient. Instead, patient-derived fibroblasts exhibit replication protein A (RPA) hyperphosphorylation dependent on DNA2 and WRN, indicating a role for RAD51 in ICL repair by preventing DNA2-mediated processing of repair intermediates (Wang et al., 2015). Another FA-associated RAD51 (FA-RAD51) mutation, A293T, was also reported to display sensitivity to crosslinking agents and camptothecin (Ameziane et al., 2015).

However, how FA-RAD51 mutations affect DNA replication beyond ICL repair and the exact molecular mechanism by which they alter RAD51 filaments remain unclear. Here, using *Xenopus laevis* egg extracts, we show that, upon RF stalling, FA-RAD51 mutants fail to protect nascent DNA from aberrant nucleolytic cleavage by MRE11. Reconstitution of DNA protection in vitro using synthetic DNA substrates confirmed that the defect is due to properties of the FA-RAD51 filaments. Electron microscopy with subsequent 3D reconstruction shows pronounced structural changes within the FA-RAD51 filaments, and, using a stopped-flow technique, we directly show that FA mutations markedly destabilize RAD51 nucleoprotein filaments. We reveal that prevention of ATP hydrolysis fails to stabilize FA-RAD51, due to aberrant nucleotide binding. This work thus uncovers a general mechanism by which the FA-RAD51 mutations affect protection of RF independently of ICL repair and thus underscores the importance of delicate cooperation between the FA/HR factors during DNA replication (Schlacher et al., 2012).

RESULTS

FA-RAD51 Mutants Are Defective at Protection of Stalled RF

First, we assessed whether FA-RAD51 mutations alleviate protection of nascent DNA at stalled RF using *Xenopus laevis* cell-free egg extracts—a well-established system for studying DNA

replication and genome maintenance-associated functions of proteins with a high degree of conservation between *Xenopus* and human proteins (Hoogenboom et al., 2017; Sannino et al., 2016). *Xenopus* extracts containing replicating chromatin were exposed to a short pulse of biotin-labeled dUTPs, followed by an aphidicolin (APH) treatment, and the remaining biotin in the nascent DNA was then quantified at various time points (Figure 1A) (Kolinjivadi et al., 2017). As expected, RAD51-depleted extracts showed a loss of nascent DNA (Hashimoto et al., 2010), which was inhibited by the MRE11 inhibitor mirin (Dupré et al., 2008), or the addition of recombinant human RAD51 wild-type (WT) (Figures 1B and S1A). In contrast, complementation of extracts with FA-RAD51 mutants did not prevent the loss of nascent DNA. The effect of T131P was more pronounced compared to A293T. In both cases, the loss of nascent DNA was largely rescued by mirin, confirming the nuclease-mediated processing of nascent DNA (Figures 1B and S1D).

Due to the previously reported dominant-negative effect of FA mutations, we also monitored stalled RF degradation in RAD51-nondepleted extracts supplemented with RAD51 WT or FA-RAD51. While the addition of WT did not further affect RF degradation, the presence of FA-RAD51 mutants resulted in a significant loss of nascent DNA, with T131P showing more severe defect (Figures 1C and S1E). This loss was again largely rescued by mirin. We also assessed the effect of FA-RAD51 on chromatin association in the background of endogenous RAD51. Supplementing extracts with WT or A293T resulted in an accumulation of RAD51 on chromatin (Figure S1B). On the other hand, the addition of T131P lowered the levels of RAD51 on DNA, suggesting that it might even destabilize residual endogenous RAD51.

We next monitored the impact of FA-RAD51 on the stability of single-stranded DNA (ssDNA) at reversed RF. RF stalling and reversal were induced by a prolonged treatment with APH, and nascent ssDNA in the replication intermediates assembled on streptavidin-coated plates was then detected using anti-BrdU (bromodeoxyuridine), which recognizes incorporated BrdU only in the context of ssDNA (Couch et al., 2013) (Figure 1D). Presence of the reversed RF containing ssDNA was also confirmed by a visual inspection of replication intermediates by EM (Figure 1E) as well as by a loss of the BrdU signal after depletion of a fork remodeling factor, SMARCAL1 (Bétous et al., 2012; Kolinjivadi et al., 2017) (Figure S1C). While supplementation of extracts with RAD51 WT did not interfere with the stability of reversed RF, the addition of T131P resulted in a marked loss of detected ssDNA 120 min after induction with APH (Figure 1F). Since the addition of mirin rescued observed instability of reversed RF, this excludes a possibility that the observed loss of a signal represents a defect of FA-RAD51 in the previously reported RF remodeling by RAD51 (Zellweger et al., 2015).

To gain insight into the mechanism of the RF protection defect, nuclease protection was reconstituted in vitro using synthetic DNA substrates. Purified RAD51 WT, T131P, or A293T were assembled on a fluorescently labeled 5′ overhang with biotin-streptavidin blocks followed by the addition of a yeast Mre11 nuclease. Whereas 2 μM WT was able to almost completely prevent DNA degradation, both mutants were less efficient in the DNA, with only 12% or 58% protection achieved by T131P and A293T, respectively (Figures 1G, 1H, and S1F) (Kolinjivadi et al., 2017). These results correlated with the observed levels of nascent DNA degradation, with RAD51 T131P exhibiting a more severe defect. Similar results were obtained also with human MRE11 and bacterial ExoIII nuclease possessing the same 3′-5′ directionality (Figures S1G and S1H), suggesting that prevention of DNA degradation is mediated by mechanical protection of the ssDNA/dsDNA (double-stranded DNA) junction.

FA Mutants Reveal Changes in Filament Formation

To understand how FA mutations alter RAD51 filaments, causing an observed defect in protection from nucleolytic degradation, we assessed their ability to form filaments. To this end, we performed a stopped-flow analysis of the filament formation kinetics previously established for monitoring RAD51 binding on DNA (Taylor et al., 2015). Individual RAD51 proteins were rapidly mixed with Cy3-labeled ssDNA, and the change of the Cy3 fluorescence was monitored in time (Figures 2A and S2). Corresponding to gel-shift assays, mutations did not affect amplitudes of the Cy3 fluorescence (Figures S2D and S2H–S2K). However, they affected the kinetics of RAD51-DNA binding, in particular at a low RAD51 concentration (Figures S2A–S2E). RAD51 WT caused a rapid increase in the fluorescence followed by an additional increase of the fluorescence after 10 s. This increase likely represents another phase of the filament formation and was not observed with the FA mutants (Figure 2A), indicating an aberrant filament formation.

Altered Structure of FA-RAD51 Filaments

Since both RAD51 mutants displayed altered DNA binding, we reasoned that the mutations might affect also structural properties and the conformation of the RAD51 filament. To determine potential conformational changes within the filament, we first performed an endonuclease protection assay with RAD51 filaments assembled on 61-mer ssDNA. Both FA mutations increased the accessibility of S1 endonuclease to DNA and only very slightly affected the cleavage pattern, which was observed for 1.5 μM RAD51 WT (Figures 2B, S2F, and S2G). This could suggest that the FA-RAD51 mutants might alter the structure and/or stability of the formed nucleoprotein filaments.

To further assess structural alterations of the FA-RAD51 filaments, we used negative-stain electron microscopy (EM) and 3D reconstruction of nucleoprotein filament segments. Measurements of the FA mutants assembled on 150-mer ssDNA were set in the presence of ATP and compared with the 3D reconstruction of the RAD51 WT filament (Figure 2C). The average 72-Å to 73-Å helical pitch for both RAD51 T131P and A293T was observed, which was much lower compared to the extended pitch of 108 Å for RAD51 WT (Figure 2D), indicating that FA-RAD51 mutations form compressed filaments. Using the negative-stain EM, we have also measured a length of the individual filaments. RAD51 WT formed longer filaments, with a length of 71 nm. Very long polymeric structures with mean lengths of 129 and 194 nm, presumably corresponding to the end-to-end stacking of the filaments, were also observed (Figure 2E). In contrast, both FA-RAD51 mutants formed short filaments with mean lengths of 42 and 53 nm for A293T and T131P, respectively. The fact that the T131P mutation more severely impaired DNA

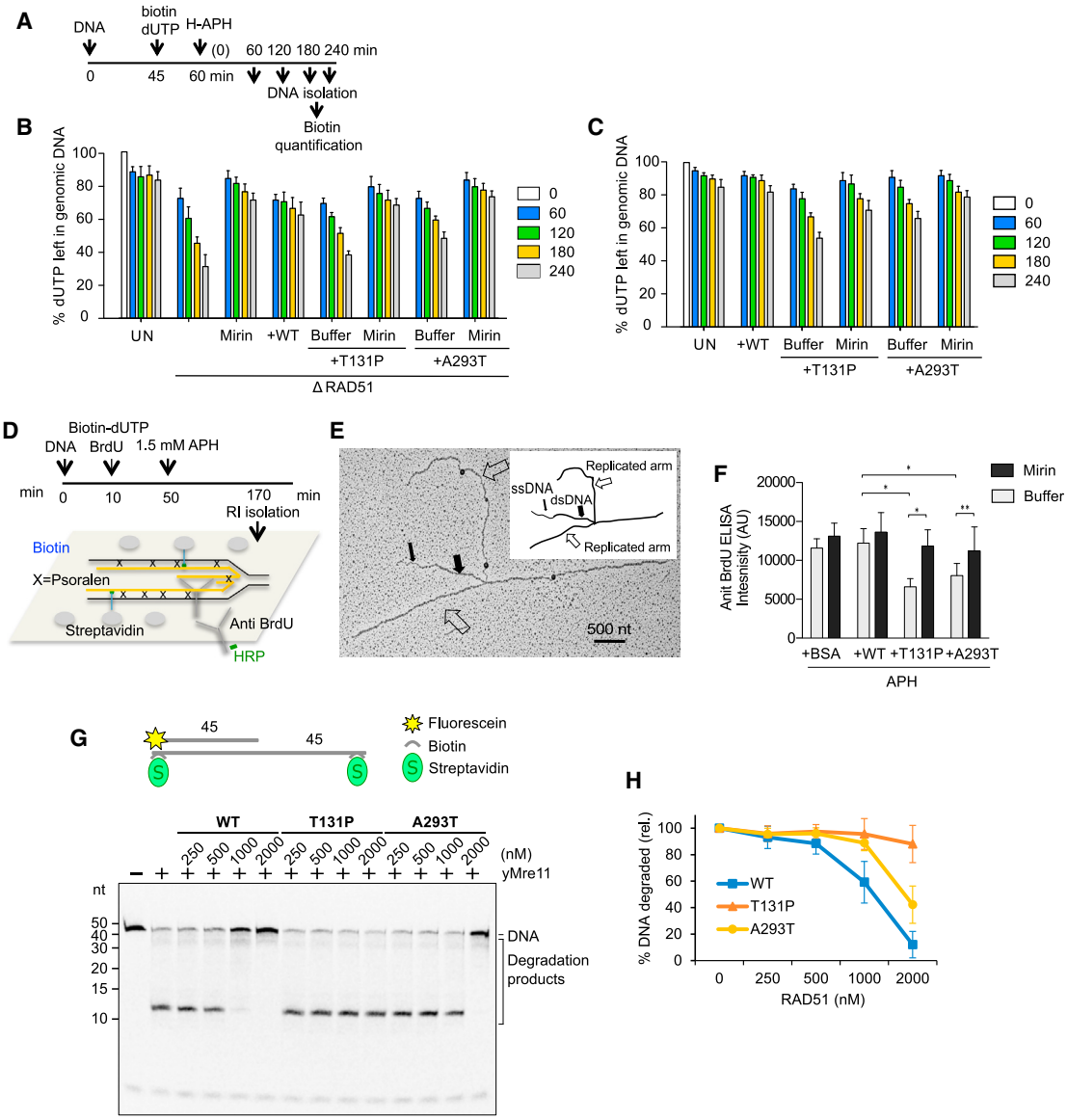

Figure 1. FA-RAD51 Mutations Impair RF Protection

(A) Scheme of the experimental set-up for (B) and (C).

(B and C) The relative percentage of residual biotin-dUTP in sperm nuclei quantified using a fluorescent method. Fluorescence intensity of mock at 0 min was considered as 100%. RAD51-depleted (A) or non-depleted (B) extracts were treated as indicated and supplemented with 100 μM mirin or indicated recombinant RAD51 proteins. Mean values ± SD (n = 3) are shown. UN, untreated.

(D) Scheme of the experimental set-up for (F). RI, replication intermediates.

(E) EM micrograph showing replication intermediates (RI) isolated 60 min after treatment with 1.5 mM APH. Open arrows indicate newly replicated strands. Arrowheads indicate regions of ssDNA and dsDNA regions of the reversed fork branch.

(F) Quantification of BrdU present in nascent ssDNA isolated at 120 min from APH addition to the extract treated as shown in (D) and detected using anti-BrdU by ELISA. Genomic DNA was isolated. Where indicated, extracts were supplemented with 5 ng/μL indicated recombinant RAD51 proteins. Mean intensity values ± SD (n = 3) are shown (*$p < 0.001$; **$p < 0.01$, Student's t test).

(G) The nuclease activity of Mre11 on streptavidin-blocked DNA substrate (5′-overhang 45-mer + 90-mer) with pre-assembled RAD51. RAD51 was assembled on a biotin-labeled fluorescent DNA substrate pre-incubated with streptavidin, followed by the addition of yMre11 (200 nM) and incubation at 30°C for 30 min. Reactions were deproteinized and resolved on 30% denaturing gel.

(H) Quantification of (G) (mean ± SD; n = 5). Rel., relatively.

See also Figure S1.

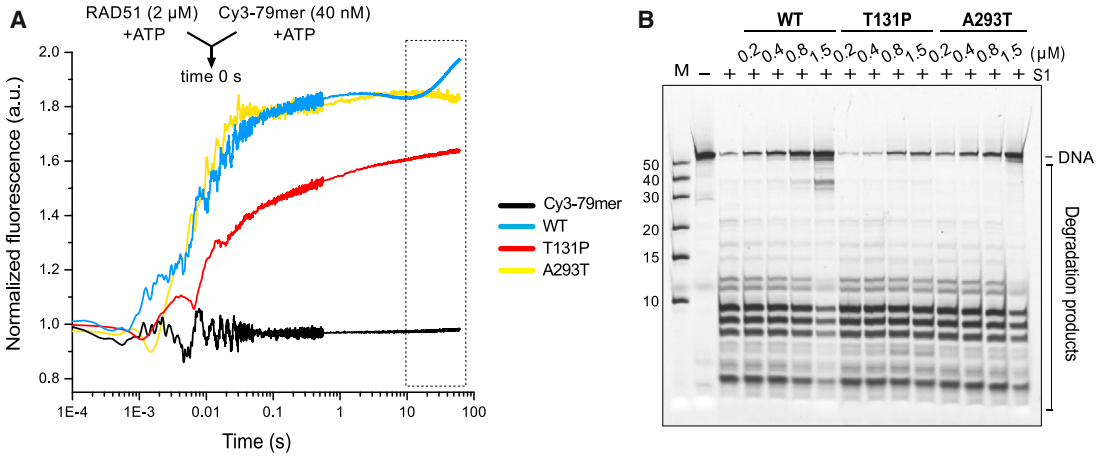

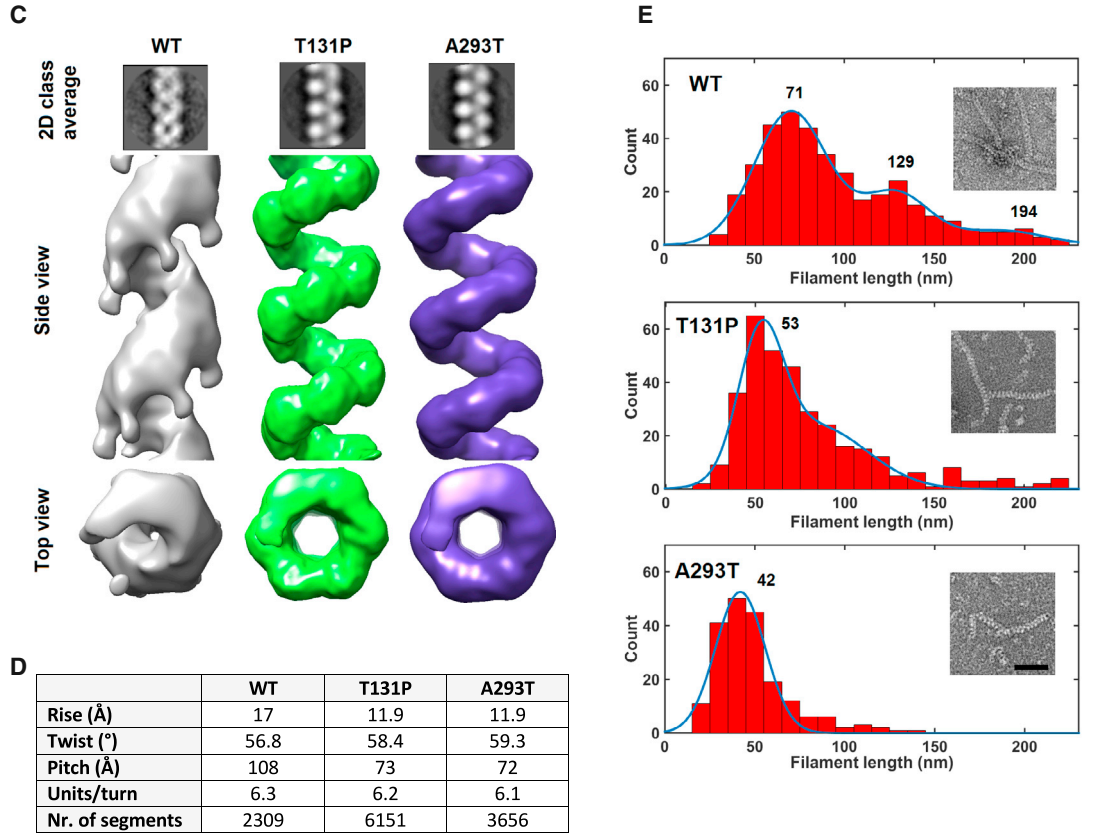

D

	WT	T131P	A293T
Rise (Å)	17	11.9	11.9
Twist (°)	56.8	58.4	59.3
Pitch (Å)	108	73	72
Units/turn	6.3	6.2	6.1
Nr. of segments	2309	6151	3656

Figure 2. Altered Formation and Structural Properties of RAD51 Nucleoprotein Filament

(A) Average normalized Cy3 fluorescence in stopped flow upon rapid mixing of RAD51 with Cy3-dT_{79} in the presence of 2 mM ATP and 10 mM $MgCl_2$. Dashed box indicates additional phase with an increase in the fluorescence observed for RAD51 WT but not FA-RAD51 mutants in time 10–60 s.

(B) RAD51 was assembled on 5′ fluorescently labeled 90-mer ssDNA followed by the addition of S1 endonuclease for 20 min at 37°C. Reactions were deproteinized and resolved on 30% denaturing gel. Quantification is shown in Figure S2G.

(C) 3D negative-stain EM reconstruction of indicated RAD51 filaments assembled on 150-mer ssDNA in the presence of 1 mM ATP and 10 mM $MgCl_2$.

(D) Table with indicated parameters from (C).

(E) Distribution of filament lengths formed by RAD51 on 150-mer in the presence of 1 mM ATP and 10 mM $MgCl_2$. Insets show examples of EM micrographs (scale bar, 50 nm).

See also Figure S2.

protection (Figure 1G), while A293T exhibited the more reduced length of RAD51 filament, might suggest that the occupancy of RAD51 at the ssDNA/dsDNA junction, rather than the filament length, is a main requirement for nuclease protection. The shortening of FA-RAD51 filaments can be explained as a direct consequence of the altered filament structure or increased RAD51 monomer dissociation, which might correlate to altered subunit self-association, demonstrated as a shift toward the formation of lower molecular weight complexes in gel filtration (Figure S3A).

FA-RAD51 Mutations Form Highly Unstable Filaments

It was previously suggested that FA-associated mutations might affect filament stability (Wang et al., 2015; Ameziane et al., 2015). We used the stopped-flow analysis to directly measure dissociation of FA-RAD51 from ssDNA. Pre-formed RAD51 WT or FA-RAD51 steady-state nucleoprotein filaments on internally labeled Cy3-dT_{43} in the presence of ATP were rapidly mixed with a 100-fold excess of unlabeled dT_{43}. Dissociation of RAD51 from labeled ssDNA results in a decrease of the fluorescent signal (Taylor et al., 2015). Compared to RAD51 WT, with a half time of dissociation 1 s, both mutants displayed dramatically increased instability, with half times of 0.01 s and 0.004 s for T131P and A293T, respectively (Figures 3A and 3F). Similar results were obtained with Cy3 label on the 5′ or 3′ end of the dT_{43} (Figures S3B–S3D), indicating that the RAD51 dissociation event occurs within the entire length of the RAD51 filament.

We also assessed filament stability with an electrophoretic mobility shift assay (EMSA) by challenging pre-formed filaments with increasing concentrations of unlabeled ssDNA (Figure 3B). In the presence of ATP and Mg^{2+} ions, T131P exhibited pronounced dissociation of the subunits from DNA, together with an altered migration pattern of the complexes (Figures 3C and 3D). In contrast to the results obtained by stopped flow, the stability of the A293T filaments was comparable to that of RAD51 WT, emphasizing the differences between the kinetics and steady-state analysis of filament stability.

Aberrant ATP Binding Destabilizes FA-RAD51 Filaments

Since the structural changes, as well as RAD51 dissociation, were shown to behave in an ATPase-dependent manner (Chi et al., 2006; Ristic et al., 2005), we next monitored RAD51 dissociation in the presence of a non-hydrolysable ATP analog, AMP-PNP. As expected, we observed stabilization of WT filament with an almost 4-fold extension of the half-time compared to that in the presence of ATP (Figures 3E and 3F). Neither of the FA-RAD51 mutations was stabilized by the prevention of ATP hydrolysis with AMP-PNP, and we even observed a slightly lower half-time of the protein-DNA complexes compared to that in the presence of ATP (Figures 3E and 3F).

We also tested AMP-PNP in the gel-based dissociation assay. In accordance, the presence of AMP-PNP resulted in almost complete RAD51 WT filament stabilization (Figures 3G and 3H). Neither T131P nor A293T was stabilized by the prevention of ATP hydrolysis. Similar results were also obtained in the presence of ATP and Ca^{2+} ions (Figures S4A and S4B), which was shown to partially prevent ATP hydrolysis (Bugreev and Mazin, 2004). Taken together, neither of the FA-RAD51 mutations increases filament stability by the prevention of ATP hydrolysis.

Since the failure to stabilize FA-RAD51 in the presence of AMP-PNP might stem from an altered ATPase catalytic cycle, we monitored ATPase activity of the FA mutants using a colorimetric ATPase assay. In contrast to WT, we observed a substantial reduction in the ATPase activity for both FA mutants (Figure 3I). To address whether the loss of the ATPase activity might reflect ATP binding, we performed a nucleotide cofactor binding assay using a ribose-modified fluorescent ATP analog, TNP-ATP. As the TNP-ATP fluorescence is enhanced upon binding within the hydrophobic nucleotide-binding site of a protein (Cheng and Koland, 1996), the fluorescence emission intensity of TNP-ATP was measured in a concentration dependency. While WT and A293T enhanced the TNP-ATP fluorescence more than 5-fold at a 2-μM concentration, the addition of T131P had almost no detectable effect on the TNP-ATP fluorescence (Figure 3J). To further confirm this observation, the kinetics of ATP binding was assessed using stopped flow by rapidly mixing a fluorophore-labeled mant-ATP analog (mATP) with RAD51 WT, which resulted in the increase of the fluorescent intensity upon mATP binding (Figure 3K). In line with our observations, T131P shows no effect in the presence of mATP (Figure 3K), and no binding was detected at any concentration tested (Figures S4C–S4E). Whereas at steady state, A293T binds ATP to the same extent as WT (Figure 3J), we observed changes in the kinetics of mATP binding (Figures 3K and S4E), suggesting aberrant ATP binding for A293T. Interestingly, while the HOP2-MND1 complex was able to facilitate optimal ATP binding of the otherwise defective RAD51 K133A mutant (Bugreev et al., 2014; Chi et al., 2006), neither of the mutants was rescued by HOP2-MND1 (Figure S4F).

Taken together, we show that alterations in ATP binding cause the improper assembly of FA-RAD51 on ssDNA, resulting in the structurally abnormal, shortened, and unstable filaments unable to properly protect RF from extensive MRE11-mediated processing.

DISCUSSION

Here, we report that two mutations associated with hereditary FA compromise RAD51's ability to prevent extensive MRE11-mediated degradation of the nascent DNA at stalled RFs. Previously, it was shown that, in the case of ICL lesions, DNA2—but not MRE11—depletion rescued extensive RPA loading at damaged sites (Wang et al., 2015). Under our experimental conditions, the addition of mirin rescued nucleolytic processing of nascent DNA strands during unperturbed replication. This is in line with our in vitro reconstitution experiments indicating that MRE11 functions in RF degradation. However, we cannot exclude that other nucleases might collaborate in DNA processing at RFs. Furthermore, the nature of the replication block should be taken into account as a crucial determining factor for the engagement of different nucleases. Distinguishing these factors remains a challenge for further studies.

The mechanistic characterization of RF protection defect revealed structural changes in the FA-RAD51 filaments and the stopped-flow analysis provided direct evidence that both FA mutations cause marked destabilization of the RAD51 filament. Importantly, we show that FA mutants are not stabilized by the

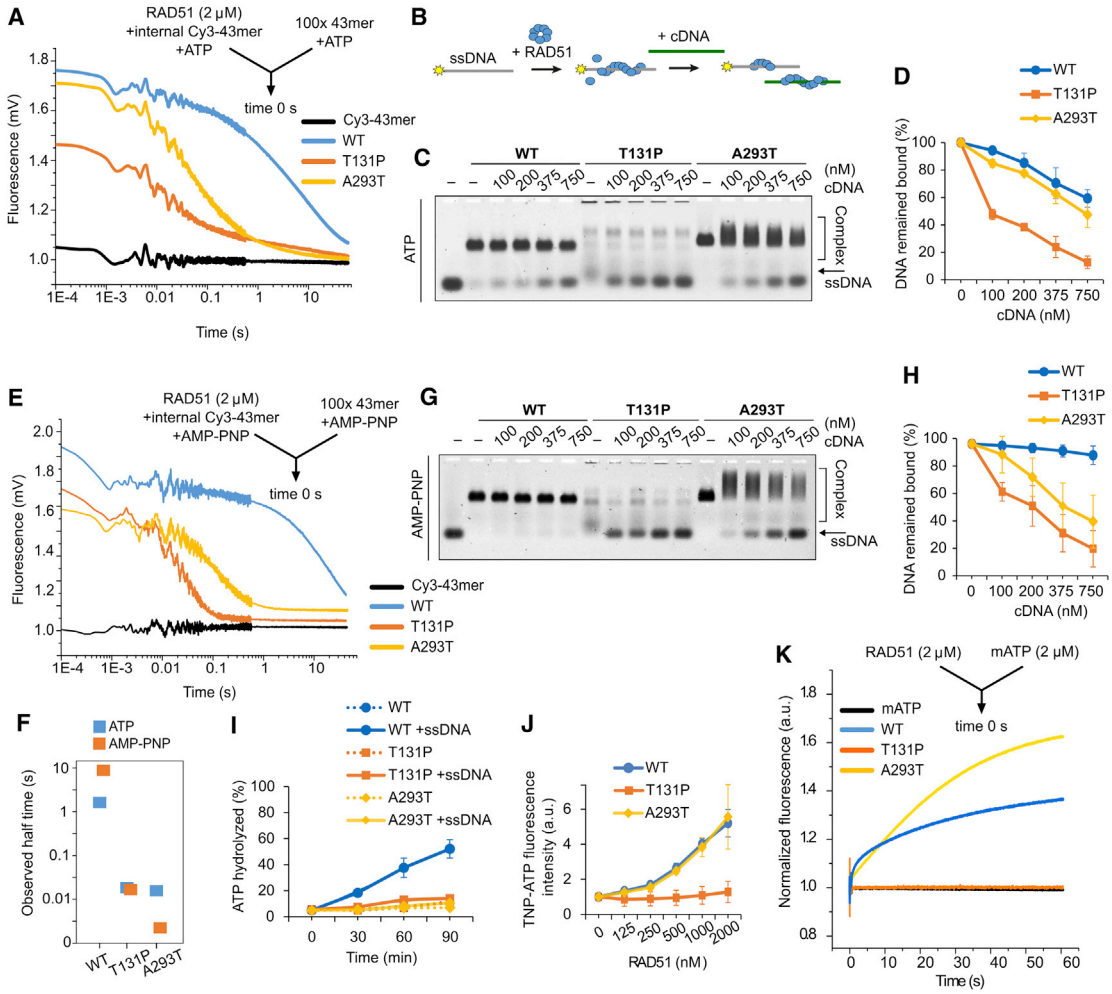

Figure 3. FA-RAD51 Filament Instability Reflects Aberrant ATP Binding and/or Hydrolysis

(A) Average Cy3 fluorescence in stopped flow upon rapid mixing of the Cy3-dT_{43}-RAD51 complex with an excess of unlabeled dT_{43} in the presence of 2 mM ATP and 10 mM $MgCl_2$.

(B) Scheme of the RAD51 filament stability experiment in (C) and (G).

(C) RAD51 was pre-incubated with fluorescently labeled 49-mer in the presence of 2 mM ATP followed by the addition of unlabeled 49-mer and incubation for 10 min at 37°C. Reactions were crosslinked and resolved on a 0.8% agarose gel.

(D) Quantification of (C) (mean ± SD; n = 3).

(E) Average Cy3 fluorescence in stopped flow upon rapid mixing of the Cy3-dT_{43}-RAD51 complex with an excess of unlabeled dT_{43} in the presence of 2 mM AMP-PNP and 10 mM $MgCl_2$.

(F) Table with indicated half times from (A) and (E).

(G) Same as in (C), except that 2 mM AMP-PNP was used in the reaction.

(H) Quantification of (F) (mean ± SD; n = 3).

(I) ATP hydrolysis measured by the colorimetric phosphate detection assay with or without 90-mer ssDNA (270 nM) in the presence of 5 mM $MgCl_2$ (mean ± SD; n = 3).

(J) ATP binding detected as a change of the fluorescence emission intensity of TNP-ATP (0.5 mM) upon binding to RAD51 in the presence of 5 mM $MgCl_2$ (mean ± SD; n = 3).

(K) Average normalized fluorescence of mATP in stopped flow upon rapid mixing with RAD51 in the presence of 10 mM $MgCl_2$.

See also Figures S3 and S4.

prevention of ATP hydrolysis as they exhibit defective or aberrant ATP binding. We did not observe substantial ATPase activity by T131P, as reported previously (Wang et al., 2015), reflecting a broader range of ATP hydrolysis measured in our assay. Our claims are additionally supported by the failure of T131P to bind the nucleotide cofactor and induce the ATP-dependent extension of B-form DNA (Ristic et al., 2005). Our data are also in line with reported ATP-dependent structural alterations for the RAD51 K133R mutant (Robertson et al., 2009) and RAD51 in the presence of nucleotide analogs (Yu et al., 2001). On the other hand, while A293T binds ATP to the same extent as WT, the kinetics of its binding suggest an aberrant conformation

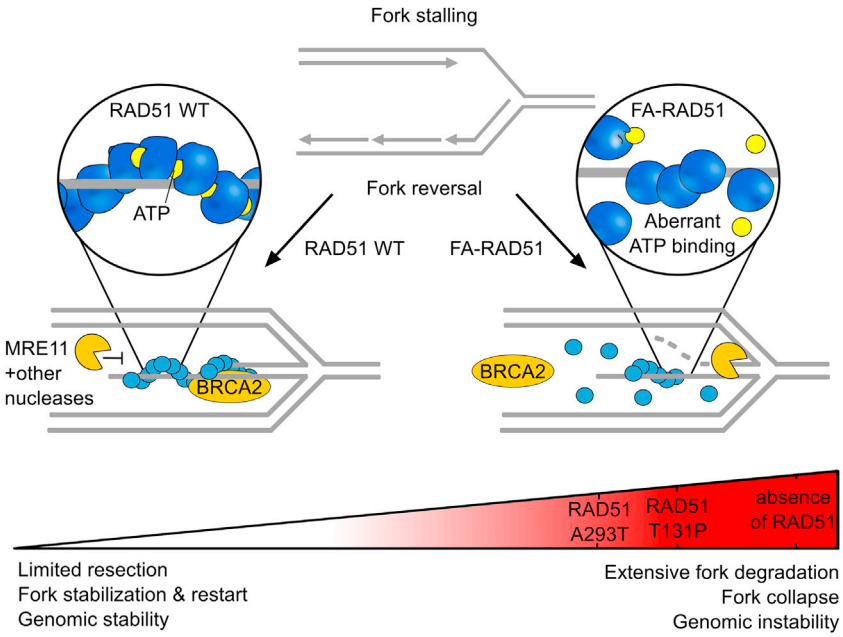

Figure 4. The Role of the RAD51 Filament in Protection of Stalled Replication Forks
See Discussion for more details.

unable to functionally activate RAD51. This also reflects a defect in ATP hydrolysis, stabilization of filament, the D-loop formation (Ameziane et al., 2015; Figures 3 and S2L), and the induction of ATP-dependent structural changes. In accordance with previous results showing a defective filament formation for the A293T mutant (Ameziane et al., 2015), we also did observe a significant defect in the filament assembly at 0.5 μM A293T, while at higher concentrations and in gel-based assays, A293T was able to saturate DNA. This, together with the dramatic instability of the A293T filament and salt sensitivity of DNA binding (Ameziane et al., 2015), points out greater protein instability in different conditions compared to RAD51 WT.

We provide evidence that RAD51 mediates protection of nascent DNA directly through blocking accessibility of the ssDNA/dsDNA junction for nuclease cleavage and highlight different requirements for RAD51 in nascent DNA protection and HR. The high rate of RAD51 dissociation compromises its ability to prevent degradation, rather than forming an active and dynamic filament required for efficient homology sampling (Bugreev et al., 2014; Taylor et al., 2015, 2016). This is in line with the observation that absence of RAD51 filament stabilization by a BRCA2 C-terminal region leads to an extensive loss of nascent DNA, whereas it is dispensable for HR (Schlacher et al., 2011). This emphasizes the importance of numerous levels of RAD51 regulation that have been uncovered (Godin et al., 2016; Krejci et al., 2012). RAD51 regulation might be essential, especially during DNA replication, when the exact timing would be required to stabilize RAD51 filaments before the release of a replication block but also promote subsequent displacement of RAD51 to permit replication progression. We hypothesize not only that FA mutant filaments are intrinsically unstable but also that aberrant ATP binding abolishes such ATP-dependent regulation (Carreira et al., 2009; Jensen et al., 2010), contributing to the observed loss of nascent DNA (Figure 4). In FA-like patient cells, the mutant proteins are expressed at a low ratio compared to RAD51 WT (Wang et al., 2015; Ameziane et al., 2015), and the defect in ATP binding might be relevant for the observed dominant-negative effect of the FA-RAD51. Incorporation of subunits with aberrantly bound ATP might trigger the distortion of the whole filament due to the lack of stabilization by mediator proteins.

While the FA-RAD51 mutations resemble RAD51 K133A mutant in vitro, which also exhibits a defect in ATP binding (Chi et al., 2006), cells expressing K133A are defective in HR (Stark et al., 2002), suggesting that these mutations might also differentially affect the interaction with RAD51 regulators in cells. In summary, our results further interconnect the FA pathway protection of RF from nucleolytic degradation and provide an insight into the molecular mechanisms of the FA-like disease development.

EXPERIMENTAL PROCEDURES

RAD51 WT, T131P, or A293T were purified from *E. coli* cells. For nascent DNA degradation, sperm nuclei (n = 4,000/μL) were incubated in 250 μL RAD51-depleted or non-depleted *Xenopus* egg extracts at 23°C supplemented with 40 nM RAD51 proteins. 45 min after the addition of the nuclei, extracts were supplemented with 40 μM biotin dUTP incubated for 15 min, and 1.5 mM APH was added. Biotin in extracted deproteinized genomic DNA was quantified. For ssDNA detection, 40 μM BrdU (Sigma) and 10 μM biotin-16-dUTP (Roche) were added to 200 μL interphase egg extracts 10 min after the addition of sperm nuclei (n = 4,000/μL). Isolated psoralen-crosslinked chromatin was deproteinized, extracted StuI-digested DNA was assembled on streptavidin-coated plates, and BrdU was detected by ELISA. For the nuclease protection assay, RAD51 was incubated for 5 min at 37°C with a fluorescein-labeled 5′ overhang (10 nM) followed by incubation with yeast Mre11 (200 nM, 30 min, 37°C). Reactions were deproteinized and resolved on 30% denaturing PAGE. The stopped flow was performed essentially as described previously (Taylor et al., 2015). For 3D reconstructions of RAD51 filaments, data were collected on a transmission electron microscope and subjected to analysis as described in the Supplemental Information. ATP hydrolysis was measured by a phosphate detection system (Innova Biosciences), with 1 μM RAD51 and 100 μM ATP in the presence or absence of ssDNA (90-mer, 270 nM). TNP-ATP binding was recorded by monitoring the fluorescence emission intensity of TNP-ATP (0.5 mM) upon preincubation with RAD51 (5 min, 37°C). Where indicated, a statistical analysis was performed in Prism software or Excel. The n represents a number of experimental replications.

SUPPLEMENTAL INFORMATION

Supplemental Information includes Supplemental Experimental Procedures and four figures and can be found with this article online at https://doi.org/10.1016/j.celrep.2017.09.062.

AUTHOR CONTRIBUTIONS

K.Z. performed most of the experiments. V.S. and V.C. designed and conducted experiments with *Xenopus leavis* extracts. K.Z., O.B., and M.S. performed stopped-flow analysis. J.M. performed EM analysis. L.K. and V.C. analyzed the data and coordinated experiments. K.Z. and L.K. wrote the manuscript.

ACKNOWLEDGMENTS

This work was funded by the Czech Science Foundation (grants GACR 17-17720S and 13-26629S), project no. LQ1605 from the National Program of Sustainability II (MEYS CR), and the Research Support Programme ([GAMU]-MUNI/M/1894/2014) to L.K.; and by the Associazione Italiana per Ricerca sul Cancro, a European Research Council Consolidator grant (614541), a Giovanni Armenise-Harvard Foundation award, the Epigen Progetto Bandiera (4.7), AICR-Worldwide Cancer Research (13-0026), and the Fondazione Telethon (GGP13-071) to V.C. V.S. is funded by a Fondazione Veronesi personal postdoctoral fellowship. We acknowledge research infrastructure projects LM2015043 and LM2015042 from MEYS CR for the financial support of the measurements at the Cryo-electron Microscopy and Tomography Core Facility and the MetaCentrum National Grid Infrastructure. We also thank J. Novacek for help with the helical reconstruction of the filaments.

Received: June 11, 2017
Revised: August 25, 2017
Accepted: September 18, 2017
Published: October 10, 2017

REFERENCES

Ameziane, N., May, P., Haitjema, A., van de Vrugt, H.J., van Rossum-Fikkert, S.E., Ristic, D., Williams, G.J., Balk, J., Rockx, D., Li, H., et al. (2015). A novel Fanconi anaemia subtype associated with a dominant-negative mutation in RAD51. Nat. Commun. *6*, 8829.

Bétous, R., Mason, A.C., Rambo, R.P., Bansbach, C.E., Badu-Nkansah, A., Sirbu, B.M., Eichman, B.F., and Cortez, D. (2012). SMARCAL1 catalyzes fork regression and Holliday junction migration to maintain genome stability during DNA replication. Genes Dev. *26*, 151–162.

Bugreev, D.V., and Mazin, A.V. (2004). Ca2+ activates human homologous recombination protein Rad51 by modulating its ATPase activity. Proc. Natl. Acad. Sci. USA *101*, 9988–9993.

Bugreev, D.V., Huang, F., Mazina, O.M., Pezza, R.J., Voloshin, O.N., Camerini-Otero, R.D., and Mazin, A.V. (2014). HOP2-MND1 modulates RAD51 binding to nucleotides and DNA. Nat. Commun. *5*, 4198.

Carreira, A., Hilario, J., Amitani, I., Baskin, R.J., Shivji, M.K.K., Venkitaraman, A.R., and Kowalczykowski, S.C. (2009). The BRC repeats of BRCA2 modulate the DNA-binding selectivity of RAD51. Cell *136*, 1032–1043.

Ceccaldi, R., Sarangi, P., and D'Andrea, A.D. (2016). The Fanconi anaemia pathway: new players and new functions. Nat. Rev. Mol. Cell Biol. *17*, 337–349.

Cheng, K., and Koland, J.G. (1996). Nucleotide binding by the epidermal growth factor receptor protein-tyrosine kinase. Trinitrophenyl-ATP as a spectroscopic probe. J. Biol. Chem. *271*, 311–318.

Chi, P., Van Komen, S., Sehorn, M.G., Sigurdsson, S., and Sung, P. (2006). Roles of ATP binding and ATP hydrolysis in human Rad51 recombinase function. DNA Repair (Amst.) *5*, 381–391.

Couch, F.B., Bansbach, C.E., Driscoll, R., Luzwick, J.W., Glick, G.G., Bétous, R., Carroll, C.M., Jung, S.Y., Qin, J., Cimprich, K.A., and Cortez, D. (2013). ATR phosphorylates SMARCAL1 to prevent replication fork collapse. Genes Dev. *27*, 1610–1623.

Dupré, A., Boyer-Chatenet, L., Sattler, R.M., Modi, A.P., Lee, J.-H., Nicolette, M.L., Kopelovich, L., Jasin, M., Baer, R., Paull, T.T., and Gautier, J. (2008). A forward chemical genetic screen reveals an inhibitor of the Mre11-Rad50-Nbs1 complex. Nat. Chem. Biol. *4*, 119–125.

Godin, S.K., Sullivan, M.R., and Bernstein, K.A. (2016). Novel insights into RAD51 activity and regulation during homologous recombination and DNA replication. Biochem. Cell Biol. *94*, 407–418.

Hashimoto, Y., Ray Chaudhuri, A., Lopes, M., and Costanzo, V. (2010). Rad51 protects nascent DNA from Mre11-dependent degradation and promotes continuous DNA synthesis. Nat. Struct. Mol. Biol. *17*, 1305–1311.

Hoogenboom, W.S., Klein Douwel, D., and Knipscheer, P. (2017). *Xenopus* egg extract: A powerful tool to study genome maintenance mechanisms. Dev. Biol. *428*, 300–309.

Jensen, R.B., Carreira, A., and Kowalczykowski, S.C. (2010). Purified human BRCA2 stimulates RAD51-mediated recombination. Nature *467*, 678–683.

Kolinjivadi, A.M., Sannino, V., De Antoni, A., Zadorozhny, K., Kilkenny, M., Técher, H., Baldi, G., Shen, R., Ciccia, A., Pellegrini, L., et al. (2017). Smarcal1-mediated fork reversal triggers Mre11-dependent degradation of nascent DNA in the absence of Brca2 and stable Rad51 nucleofilaments. Mol. Cell *67*, 867–881.e7.

Krejci, L., Altmannova, V., Spirek, M., and Zhao, X. (2012). Homologous recombination and its regulation. Nucleic Acids Res. *40*, 5795–5818.

Long, D.T., Räschle, M., Joukov, V., and Walter, J.C. (2011). Mechanism of RAD51-dependent DNA interstrand cross-link repair. Science *333*, 84–87.

Räschle, M., Knipscheer, P., Enoiu, M., Angelov, T., Sun, J., Griffith, J.D., Ellenberger, T.E., Schärer, O.D., and Walter, J.C. (2008). Mechanism of replication-coupled DNA interstrand crosslink repair. Cell *134*, 969–980.

Ristic, D., Modesti, M., van der Heijden, T., van Noort, J., Dekker, C., Kanaar, R., and Wyman, C. (2005). Human Rad51 filaments on double- and single-stranded DNA: correlating regular and irregular forms with recombination function. Nucleic Acids Res. *33*, 3292–3302.

Robertson, R.B., Moses, D.N., Kwon, Y., Chan, P., Chi, P., Klein, H., Sung, P., and Greene, E.C. (2009). Structural transitions within human Rad51 nucleoprotein filaments. Proc. Natl. Acad. Sci. USA *106*, 12688–12693.

Sannino, V., Kolinjivadi, A.M., Baldi, G., and Costanzo, V. (2016). Studying essential DNA metabolism proteins in *Xenopus* egg extract. Int. J. Dev. Biol. *60*, 221–227.

Schlacher, K., Christ, N., Siaud, N., Egashira, A., Wu, H., and Jasin, M. (2011). Double-strand break repair-independent role for BRCA2 in blocking stalled replication fork degradation by MRE11. Cell *145*, 529–542.

Schlacher, K., Wu, H., and Jasin, M. (2012). A distinct replication fork protection pathway connects Fanconi anemia tumor suppressors to RAD51-BRCA1/2. Cancer Cell *22*, 106–116.

Stark, J.M., Hu, P., Pierce, A.J., Moynahan, M.E., Ellis, N., and Jasin, M. (2002). ATP hydrolysis by mammalian RAD51 has a key role during homology-directed DNA repair. J. Biol. Chem. *277*, 20185–20194.

Taylor, M.R.G., Špírek, M., Chaurasiya, K.R., Ward, J.D., Carzaniga, R., Yu, X., Egelman, E.H., Collinson, L.M., Rueda, D., Krejci, L., and Boulton, S.J. (2015). Rad51 paralogs remodel pre-synaptic Rad51 filaments to stimulate homologous recombination. Cell *162*, 271–286.

Taylor, M.R.G., Špírek, M., Jian Ma, C., Carzaniga, R., Takaki, T., Collinson, L.M., Greene, E.C., Krejci, L., and Boulton, S.J. (2016). A polar and nucleotide-dependent mechanism of action for RAD51 paralogs in RAD51 filament remodeling. Mol. Cell *64*, 926–939.

Wang, A.T., Kim, T., Wagner, J.E., Conti, B.A., Lach, F.P., Huang, A.L., Molina, H., Sanborn, E.M., Zierhut, H., Cornes, B.K., et al. (2015). A dominant mutation in human RAD51 reveals its function in DNA interstrand crosslink repair independent of homologous recombination. Mol. Cell *59*, 478–490.

Yu, X., Jacobs, S.A., West, S.C., Ogawa, T., and Egelman, E.H. (2001). Domain structure and dynamics in the helical filaments formed by RecA and Rad51 on DNA. Proc. Natl. Acad. Sci. USA *98*, 8419–8424.

Zellweger, R., Dalcher, D., Mutreja, K., Berti, M., Schmid, J.A., Herrador, R., Vindigni, A., and Lopes, M. (2015). Rad51-mediated replication fork reversal is a global response to genotoxic treatments in human cells. J. Cell Biol. *208*, 563–579.